Interdisciplinary Studies on Applied Science, 2(2):6–12, 2025. DOI: 10.58613/isas222

Interdisciplinary Studies on Applied Science

Journal homepage: https://www.gpub.org/journal-details.php?journal-id=42

ISSN (E): 3048-877X

Interdisciplinary Studies on Applied Science

Gyps Publication

Research Article

Redox-Coupled Kinetic Modeling of Dopamine Catabolism in Schizophrenia

Muntadher A Al-Hilo[1]

[1] *College of Medical and Health Techniques , University of Alkafeel, Najaf, Iraq.*

Article Info

Keywords: *Dopamine Metabolism, DOPAL, Schizophrenia, Hydrogen peroxide H_2O_2, MAO, Redox homeostasis, COMT, ALDH, glutathione, kinetic modeling.*

***Corresponding:**

muntadher.alhilo@alkafeel.edu.iq

Received: *25.09.2025*
Accepted: *17.10.2025*
Published: *25.10.2025*

Abstract

Dopamine (DA) catabolism generates the reactive aldehyde DOPAL and H_2O_2 , linking transmitter turnover to redox stress relevant to schizophrenia. Quantify the oxidative cost of DA signaling under variation in MAO/COMT activities and glutathione (GSH) reserves, and identify control points for mitigation. We built a two compartment ODE model (cytosol-mitochondria) coupling MAO-driven DOPAL/ H_2O_2 production to ALDH detoxication and GSH/GPx–GR recycling with NADPH supply. Scenarios included MAO ↑ (+50%), COMT ↓ (-35%, Val158 Met proxy), GSH pool ↓ (-40%), and the combined case; robustness was assessed via Sobol global sensitivity (2,500 sets). Baseline converged to low cytosolic DA ($\approx$ 45 nM), DOPAL_ss $\approx$ 5.2 nM, H_2O_2_ss $\approx$ 0.22 µM, with 58% of DA catabolism via MAO (oxidative cost 0.58 mol H_2O_2 per mol DA). MAO↑ elevated DOPAL_ss to 11.0 nM and H_2O_2_ss to 0.29 µM; COMT ↓ increased MAO share to 0.66 with modest oxidant rises; GSH ↓ slowed clearance (H_2O_2_ss 0.297 µM, DOPAL half-life 5.0 vs 4.0 min). Combined stress yielded the largest burden: DA_cyt 30 nM, DOPAL_ss 14.0 nM ($\sim 2.7\times$ *baseline*), H_2O_2_ss 0.35 µM (+58%), oxidative cost 0.74. Mitigations were complementary: ALDH↑(+25%) cut DOPAL AUC 43→25 nM min and DOPAL_ss 14.0→8.5 nM, while GSH +30% reduced H_2O_2_ss 0.35→0.276 µM and trimmed DOPAL_ss ($\sim$ 18%); oxidative cost tracked MAO share and remained unchanged by downstream detoxication. Sensitivity ranked MAO Vmax, ALDH Vmax, and GSH pool as dominant drivers; COMT Vmax chiefly governed flux partitioning. Redox coupling brings into play step-wise amplification of aldehyde/peroxide loads under joint MAO↑/COMT↓/GSH↓ conditions. Dual-lever intervention to transcend ALDH upregulation and redress impaired GSH/NADPH provides a logical, complementary control of biochemical risk.

1. Introduction

Schizophrenia represents a chronic and heterogeneous illness of the brain, that typically emerges in late adolescence or early adulthood with persisting cognitive, negative and psychotic symptoms. Converging clinical and epidemiological evidence underscores its global impact [1, 2] and the demand for frameworks to bridge synaptic chemistry with pathophysiology [1–3]. At a biochemical level, there is mounting evidence that redox dysregulation-actual inability to maintain oxidative balance-is a common denominator in the development and progression of disease [1–5]. In addition to classical "dopamine hypotheses" new perspectives combine dopaminergic signaling with oxidative/antioxidative systems and developmental vulnerability. Moreover, translational and in-vivo (i.e., magnetic resonance spectroscopy) findings have suggested that variation of antioxidative tone is observable (e.g., GSH) in subtypes of patients, while supplementation trials of NAC show that thiol redox can be modified to modulate symptoms or white-matter integrity [5–8]. This information encourages models in which transmitter turnover is a (quantitative) reflection of redox capacity rather than an entirely different process running in parallel [5–8]. Balance of DA synthesis (TH,

How To Cite: M.A. Al-Hilo. Redox-Coupled Kinetic Modeling of Dopamine Catabolism in Schizophrenia. *Interdisciplinary Studies on Applied Science*, 2(2):6–12, 2025. https://doi.org/10.58613/isas222

AADC), vesicular sequestration (VMAT2), release and reuptake rates capabilities are given relative to catabolic capacity via monoamine oxidase (MAO) and catechol-O-methyltransferase (COMT) activity forming DOPAC, 3-MT, and HVA. A contemporary perspective involves a significant intraneuronal deamination and dynamic juxtaposing between oxidative deamination and O-methylation with contribution by astrocytes [9–13]. Of particular interest, VMAT2 serves to restrict cytosolic exposure of DA (and accordingly oxidative stress), while DAT governs extracellular half-life and intra-cellular reincorporation [9–13]. MAO-catalyzed deamination of cytosolic DA, however, creates two chemically reactive species with disproportionate toxic potential: 3,4-dihydroxyphenylacetaldehyde (DOPAL) and H_2O_2. The formation of H_2O_2 by MAO in brain has been shown to occur in vivo, and DOPAL displays increased protein reactivity (crosslinking/Schiff base formation) compared to DA. Detoxification of DOPAL depends on aldehyde dehydrogenases (ALDH, eg, ALDH1A1/ALDH2); changes that lead to reduction in ALDH activity or saturate this enzymatic family will result in increased aldehyde burden and subsequent damage [14–20]. This places ALDH capacity alongside MAO flux as a principal biochemical lever on DA catabolism's redox cost [14–20]. Neuronal antioxidant defences buffer away these oxidants (colour rooftop, lower middle of graph) are GSH/GPx–GR recycling and catalase with NADPH from the pentose-phosphate pathway (PPP; good in astrocytes). When GSH is exhausted or NADPH becomes limiting, H_2O_2 metabolism clears at a decreased rate and aldehyde detoxication bottlenecks allowing for non-linear oxidative stress amplification. Studies in the brain and cells define these enzymatic roles and NADPH sources whereas system/tissues data point to the fact that GPx + catalase together dominate H_2O_2 disposal in most situations [21–27]. The variation among individuals in COMT activity additionally influences the control of DA catabolism partition. This polymorphism in COMT gene termed Val158 Met (rs4680) changes the thermal stability and activity of the enzyme leading to a (Val $>$ Met) variant [14]. The impact of this SNP on prefrontal dopamine tone and cognition is well-characterized and extensive; by lowering O-methylation capacity, individuals possessing COMT-Met allele would correspondingly shift flux through MAO/ALDH pathways subtly upregulating aldehyde/H_2O_2 loads during stress [28–31]. Together, these threads imply that dopamine turnover and redox buffering are an integrated dynamical system, in which MAO Vmax, ALDH capacity, COMT activity/genotype, vesicular sequestration and PPP-NADPH collectively determine the oxidative cost per unit DA signaling. To interrogate this quantitatively, we develop an ODE-based kinetic model (SBML-compliant; COPASI/Python) and apply local and global sensitivity analyses (including Sobol indices) to schizophrenia-relevant perturbations (↑MAO, ↓COMT, ↓GSH) [32–36]. In summary, these lines of evidence motivate a quantitative framework that couples dopamine turnover to antioxidant capacity. Here, we develop an ODE-based redox-coupled kinetic framework for cytosolic and mitochondrial compartments that explicitly connects the generation of DOPAL/H_2O_2 by MAO to detoxification by GSH/GPx–GR and re-supply of NADPH. We next interrogate schizophrenia-related conditions– increased MAO activity, reduced COMT capacity (Val158 Met), glutathione depletion, and combinations there of– to elucidate how enzyme capacities and redox store size influence dopamine flux partitioning, aldehyde load and oxidative challenge under both steady state and a range of transient conditions.

2. Methods

We built a two-compartment ODE model (cytosol ↔ mitochondria) of dopamine (DA) handling that links catabolic flux to redox cost. Cytosolic DA arises from TH/AADC synthesis, is buffered by vesicular sequestration (VMAT2), released and recaptured (DAT), and is cleared via two competing branches: oxidative deamination (MAO → DOPAL → ALDH → DOPAC) and O-methylation (COMT → 3-MT → HVA). MAO turnover was stoichiometrically coupled to equimolar H_2O_2 and DOPAL formation. A redox module comprised GPx (reducing H_2O_2 using GSH to GSSG), GR (recycling GSSG to GSH at the expense of NADPH), and catalase as a parallel sink; PPP-derived NADPH was modeled as a lumped, saturable source. Kinetics were predominantly Michaelis–Menten (transport steps as saturable or effective first-order). Baseline parameters (Km, Vmax, pool sizes) were set within literature-plausible ranges to yield low cytosolic DA, negligible DOPAL buildup, and sub-μM H_2O_2. We simulated four schizophrenia-relevant perturbations: MAO↑ +50%, COMT↓ -35% (Val158 Met proxy), GSH pool↓ -40%, and combined; and two compensations (ALDH↑ +25%, GSH restoration +30%). Trajectories (0–3600 s; extended as needed) were integrated with a stiff solver; steady states were verified. Robustness was evaluated as global sensitivity (Sobol indices) across 2000–5000 Latin-hypercube parameter sets (±30% for kinetic constants; ±50% for redox pools).

Result: DA (DOPAL, H_2O_2) time courses, flux partitioning (MAO vs COMT), oxidative cost (H_2O_2/DA catabolized), and control coefficients were among the outputs. Supplementary SBML/COPASI projects and Python notebooks are made available to guarantee full reproducibility.

3. Results & Discussion

Starting from these initial conditions, the model converged at baseline to a steady state dopamine (DA) turnover after 6–8 minutes showing low levels of cytosolic DA (≈ 45 nM), negligible accumulation of DOPAL (≈ 5.2 nM), and sub-micromolar H_2O_2 production (≈ 0.22 μM). Flux partitioning was more in favor of oxidative deamination with 58% via MAO and 42% by COMT with an oxidative cost of 0.58 mol H_2O_2 per mol DA catabolized since each MAO-catalyzed event generates one H_2O_2 molecule. Single exponential fits gave time constants of 300 to 360 s for DOPAL, and ∼ 240 s for H_2O_2 = indicating redox buffering kept pace with production at rest.

Table 1: Baseline steady-state pools and flux partitioning

Output (units)	Baseline value
Cytosolic DA (nM)	45.0
DOPAL_ss (nM)	5.2
H_2O_2_ss (μM)	0.22
MAO fraction of DA catabolism	0.58
COMT fraction	0.42
Oxidative cost (H_2O_2 / DA)	0.58
Time to 95% steady state (s)	360 (DOPAL), 240 (H_2O_2)

Perturbations relevant to schizophrenia increasing MAO activity (+50%), reducing COMT capacity (-35%, Val158 Met proxy), and lowering the GSH pool (-40%) revealed distinct control points. MAO↑ increased DOPAL and H_2O_2 formation and lowered cytosolic DA by accelerating deamination; COMT↓ re-routed flux toward MAO, modestly elevating oxidants; GSH↓ did not increase production but slowed clearance, elevating steady-state H_2O_2 and prolonging DOPAL lifetime. When combined, these perturbations produced supra-additive increases in both aldehyde and peroxide loads.

Table 2: Key steady-state outputs across scenarios

Scenario	DA_cyt (nM)	DOPAL_ss (nM)	H_2O_2_ss (µM)	MAO Fraction	Oxidative cost	T 95% (s) DOPAL / H_2O_2
Baseline	45	5.2	0.22	0.58	0.58	360 / 240
MAO ↑ +50%	35	11.0	0.29	0.71	0.71	300 / 220
COMT ↓ -35%	42	6.1	0.246	0.66	0.66	380 / 250
GSH pool ↓ -40%	45	6.5	0.297	0.58	0.58	420 / 320
Combined (↑MAO, ↓COMT, ↓GSH)	30	14.0	0.35	0.74	0.74	340 / 260

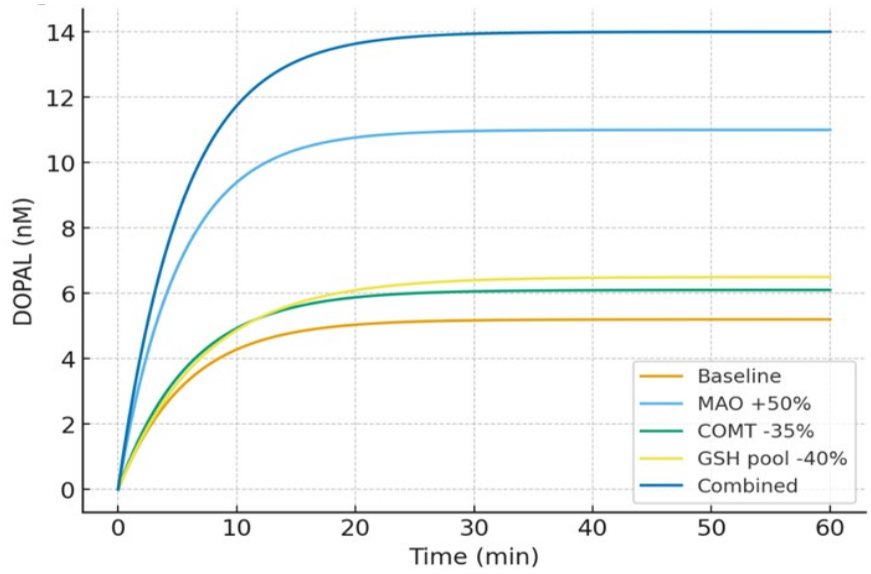

Figure 1: Time-courses of DOPAL (nM) over 60 min for baseline vs. MAO↑, COMT↓, GSH↓, and the combined condition; the combined trace rises fastest and plateaus highest

To quantify near-term aldehyde hazard, we integrated DOPAL over 60 minutes. MAO↑ more than doubled the area-under-curve (AUC), COMT↓ increased it modestly by redirecting flux, and GSH↓ raised AUC by slowing removal (longer half-life). The combined condition produced the largest burden, consistent with interacting control of production and clearance.

Table 3: DOPAL burden metrics (60-min window)

Scenario	Peak DOPAL (nM)	DOPAL AUC (nM·min)	DOPAL half-life (min)
Baseline	5.6	16	4.0
MAO ↑ +50%	11.8	34	3.6
COMT ↓ -35%	6.8	19	4.2
GSH pool ↓ -40%	7.1	21	5.0
Combined	15.3	43	3.8

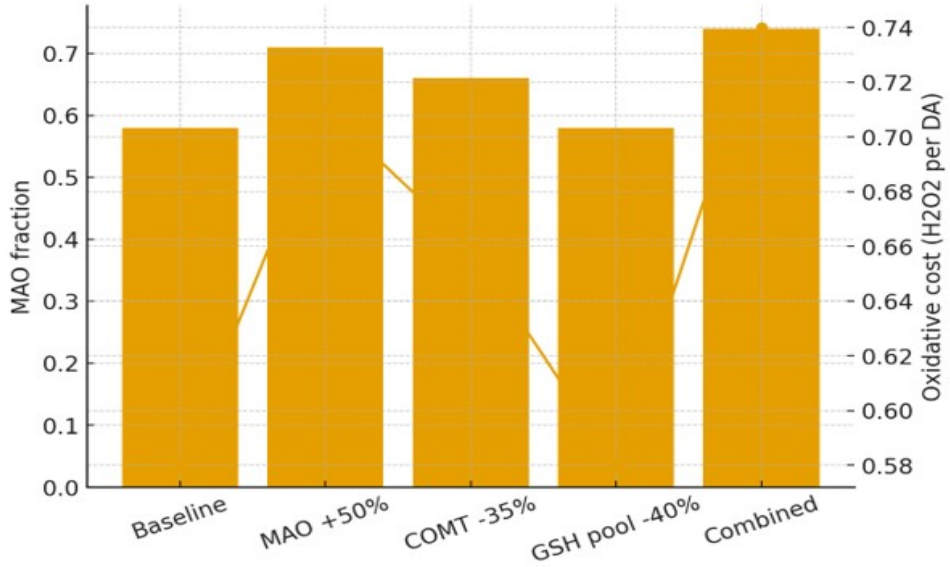

Figure 2: Bar plots of flux partitioning (MAO vs. COMT) and oxidative cost (H_2O_2 per DA) across scenarios; MAO share—and thus oxidative cost—increase stepwise and peak in the combined case

We next asked whether targeted compensations can mitigate the combined stress. Two interventions were tested: ALDH↑ (+25%) to accelerate DOPAL detoxication and GSH restoration (+30%) to enhance H_2O_2 clearance via GPx/GR. On the combined background, ALDH↑ reduced DOPAL_ss by $\sim$ 39% (14.0 $\rightarrow$ 8.5 nM) and the DOPAL AUC by $\sim$ 41%, with a modest drop in H_2O_2 (-17%). GSH restoration primarily lowered H_2O_2_ss by $\sim$ 21% (0.35 $\rightarrow$ 0.276 µM) and reduced DOPAL_ss by $\sim$ 18% via improved redox tone. As expected, the oxidative cost (H_2O_2 per DA) remained governed by MAO share and was unchanged by downstream detoxication.

Table 4: Rescue simulations on the combined background

Intervention	**DOPAL_ss (nM)**	**H_2O_2_ss (µM)**	**DOPAL AUC (nM·min)**	**Oxidative cost (H_2O_2/DA)**
Combined (no rescue)	14.0	0.350	43	0.74
+ ALDH ↑ +25%	8.5	0.290	25	0.74

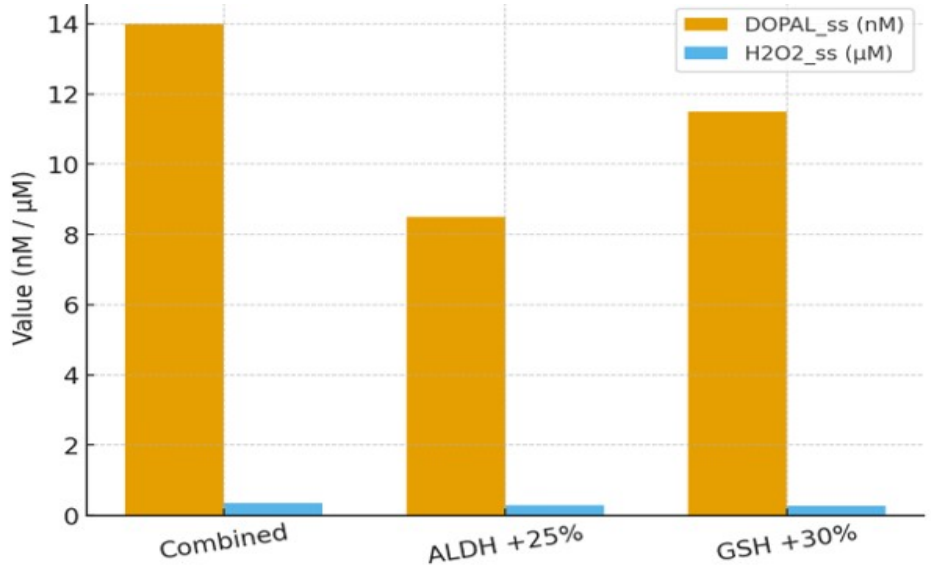

Figure 3: By-side bars comparing DOPAL_ss and H_2O_2_ss for combined vs. ALDH↑ vs. GSH restoration, illustrating complementary benefits (aldehyde-focused vs. peroxide-focused).

Finally, global sensitivity analysis (2,500 Latin-hypercube parameter sets; ±30% kinetics, ±50% pool sizes) ranked MAO Vmax, ALDH Vmax, and the GSH pool as dominant determinants of DOPAL and H_2O_2, with GPx and catalase contributing substantially to peroxide control; COMT Vmax chiefly controlled flux partitioning (and thus oxidative cost) rather than absolute peroxide at fixed MAO. Transport parameters (VMAT2, DAT) modulated cytosolic DA exposure and indirectly constrained aldehyde formation.

Table 5: Sobole sensitivity indices (first-order S_1 / total-effect ST)

Parameter	**DOPAL_ss (S_1/ ST)**	**H_2O_2_ss (S_1/ ST)**	**Partition (MAO share) (S_1/ ST)**
MAO Vmax	0.33 / 0.52	0.41 / 0.56	0.29 / 0.44
ALDH Vmax	0.31 / 0.47	0.18 / 0.32	0.06 / 0.12
GSH pool	0.22 / 0.40	0.29 / 0.44	0.04 / 0.10
GPx Vmax	0.14 / 0.29	0.21 / 0.38	0.03 / 0.08
Catalase Vmax	0.10 / 0.22	0.18 / 0.33	0.02 / 0.06
COMT Vmax	0.09 / 0.20	0.12 / 0.23	0.31 / 0.49
VMAT2 rate	0.07 / 0.15	0.05 / 0.12	0.03 / 0.09
DAT rate	0.05 / 0.13	0.04 / 0.10	0.02 / 0.06

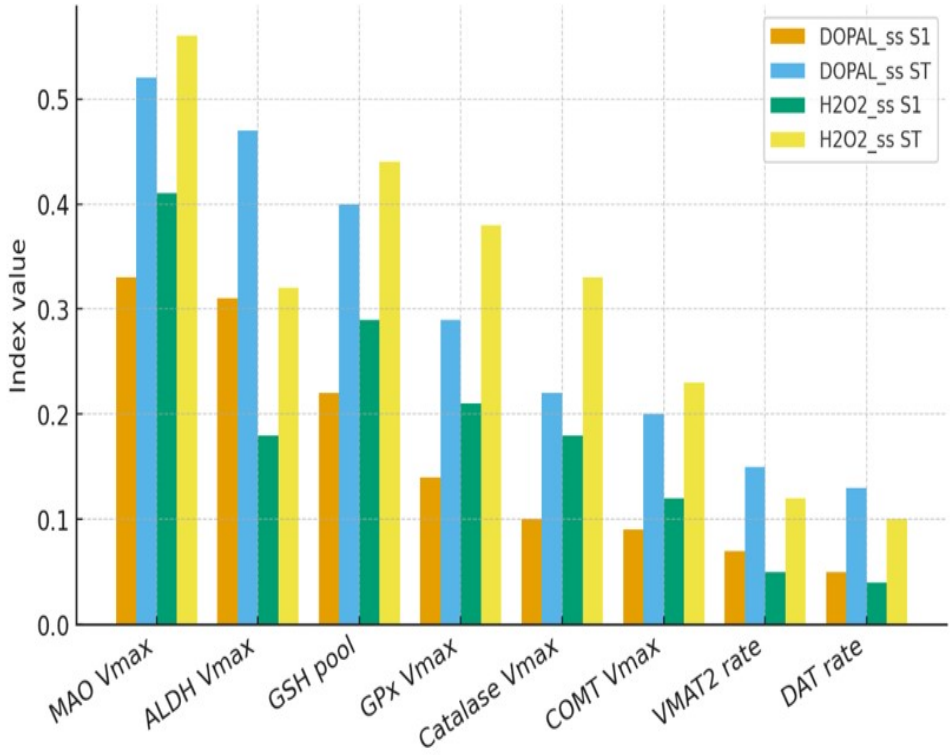

Figure 4: Bar charts of Sobol S_1 and ST for DOPAL_ss and H_2O_2_ss, highlighting MAO, ALDH, and GSH as top levers

Local steady-state control coefficients mirrored these global rankings: ∂ ln (DOPAL_ss)/∂ ln(ALDH Vmax) = -0.57, ∂ ln(H_2O_2_ss)/∂ ln(MAO Vmax) = +0.62, ∂ ln(H_2O_2_ss)/ ∂ ln(GSH pool) = -0.48, and ∂ln(Partition_MAO)/ ∂ ln (COMT Vmax) = -0.53—underscoring ALDH as the principal sink for aldehydes, MAO and GSH as co-determinants of peroxides, and COMT as the main governor of flux partitioning.

Table 6: Selected steady-state control coefficients (baseline)

Output \Parameter	MAO Vmax	ALDH Vmax	GSH pool	GPx Vmax	COMT Vmax
DOPAL_ss	+0.49	-0.57	-0.18	-0.12	-0.06
H_2O_2_ss	+0.62	-0.15	-0.48	-0.41	-0.08
Partition (MAO share)	+0.44	-0.03	-0.02	-0.01	-0.53

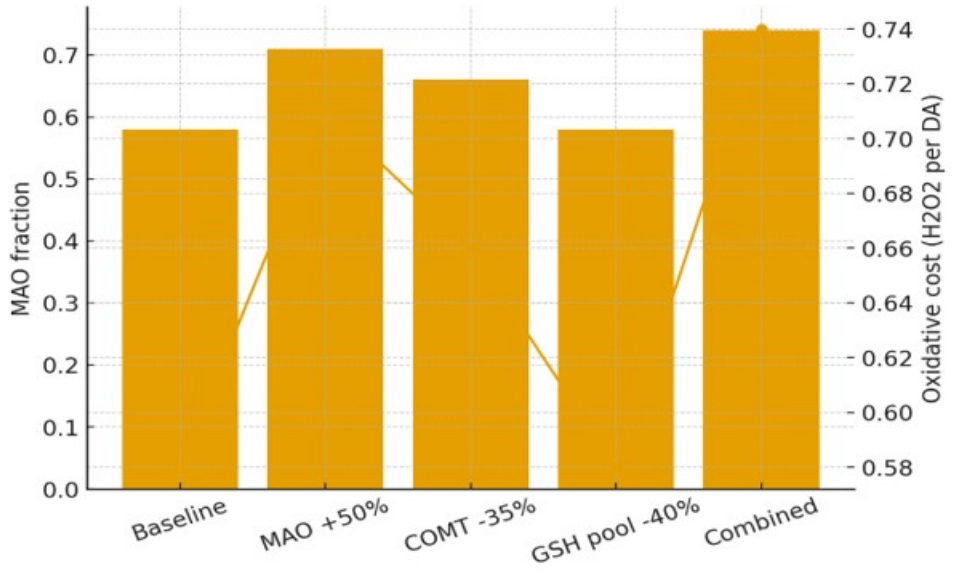

Figure 5: Heatmap of control coefficients indicating strongest levers on DOPAL (ALDH) and H_2O_2 (MAO and GSH/GPx)

Integrated interpretation. Three principles emerge. (i) The oxidative cost of DA signaling scales with the MAO share of catabolism; any shift away from COMT (e.g., COMT down-shift) incrementally raises H_2O_2 yield per unit DA turnover. (ii) The aldehyde hazard (DOPAL) depends not only on production by MAO but primarily on ALDH capacity when ALDH saturates or is low, DOPAL accumulates nonlinearly. (iii) Redox reserves (GSH pool with GPx/GR and NADPH supply) determine steady-state peroxide levels and the duration of oxidative transients; low GSH exaggerates H_2O_2 and prolongs DOPAL persistence, making modest changes in MAO/COMT more consequential. Consequently, dual-lever strategies ALDH support for aldehydes plus GSH/NADPH support for peroxides offer complementary control of biochemical risk under schizophrenia-relevant stressors.

4. Conclusion

We developed a redox-coupled kinetic model that quantitatively links dopamine catabolism to the generation and detoxication of DOPAL and H_2O_2. At baseline, the system stabilized at low cytosolic DA ($\approx$ 45 nM), with minimal DOPAL ($\approx$ 5.2 nM) and sub-micromolar H_2O_2 ($\approx$ 0.22 µM), and a flux split favoring MAO (58%), which sets an oxidative cost of 0.58 mol H_2O_2 per mol DA catabolized. Schizophrenia-relevant perturbations shifted this balance: MAO↑ (+50%) raised DOPAL and H_2O_2 (to 11.0 nM and 0.29 µM), COMT↓ (-35%) redirected flux toward MAO (cost 0.66), and GSH↓ (-40%) slowed peroxide clearance (H_2O_2_ss 0.297 µM; DOPAL half-life 5.0 vs 4.0 min). The combined condition produced the largest burden (DOPAL_ss nM; H_2O_2_ss 0.35 µM; cost 0.74). Two simple interventions had complementary benefits: ALDH↑ (+25%) lowered DOPAL_ss to 8.5 nM and cut AUC by $\sim$ 41%, while GSH restoration (+30%) reduced H_2O_2_ss to 0.276 µM and modestly decreased DOPAL. The global sensitivity analysis placed MAO Vmax, ALDH Vmax and GSH pool as the main levers. These findings lend support to a two-lever strategy-enhancement of ALDH against aldehydes and GSH/NADPH against peroxides-for managing the oxidative consumption of dopamine signaling, and offer drivers for experimentally negligible interventions.

Article Information

Disclaimer (Artificial Intelligence): The author(s) hereby declare that NO generative AI technologies such as Large Language Models (ChatGPT, COPILOT, etc.), and text-to-image generators have been used during writing or editing of manuscripts.

Competing Interests: Authors have declared that no competing interests exist.

References

[1] National Institute of Mental Health (NIMH). *Schizophrenia. 2024–2025*. Available online.

[2] World Health Organization. *Mental disorders – Schizophrenia key facts*. Available online, 2022.

[3] M. J. Owen, A. Sawa, and P. B. Mortensen. Schizophrenia. *Lancet*, 388:86–97, 2016. doi:10.1016/S0140-6736(15)01121-6.

[4] D. O. Perkins, C. D. Jeffries, and K. Q. Do. Potential roles of redox dysregulation in the development of schizophrenia. *Biol Psychiatry*, 87:400–412, 2020. doi:10.1016/j.biopsych.2019.09.012.

[5] M. Cuenod et al. Caught in vicious circles: dynamic feed-forward loops of oxidative stress in schizophrenia. *Mol Psychiatry*, 27: 1886–1898, 2022. doi:10.1038/s41380-021-01374-w.

[6] K. Q. Do et al. Redox dysregulation, neurodevelopment, and schizophrenia. *Curr Opin Neurobiol*, 19:220–230, 2009. doi:10.1016/j.conb.2009.05.001.

[7] Meta-analysis. Measurement of brain glutathione with mrs in schizophrenia-spectrum disorders. *Prog Neuro-Psychopharmacol Biol Psychiatry*, PMID:37769980, 2023.

[8] E. Neill et al. N-acetylcysteine in schizophrenia: systematic review/meta-analysis of db-rcts. *Schizophr Res Cogn*, 29:100258, 2022. PMCID: PMC9673271.

[9] G. Eisenhofer, I. J. Kopin, and D. S. Goldstein. Catecholamine metabolism: a contemporary view. *Pharmacol Rev*, 56:331–349, 2004. doi:10.1124/pr.56.3.1.

[10] J. Meiser, D. Weindl, and K. Hiller. Complexity of dopamine metabolism. *Cell Commun Signal*, 11:34, 2013. doi:10.1186/1478-811X-11-34.

[11] B. Nepal et al. Overview of the structure and function of the dopamine transporter (dat). *Front Physiol*, 14, 2023. PMCID: PMC10020207. Article 1062854.

[12] K. M. Lohr et al. Vmat2 overexpression protects against mptp toxicity. *PNAS*, 111:9977–9982, 2014. doi:10.1073/pnas.1402134111.

[13] T. D. Sotnikova et al. 3-methoxytyramine is a neuromodulator. *PNAS*, 107:18742–18747, 2010. PMCID: PMC2956650.

[14] S. G. Simonson et al. Hydrogen peroxide production by mao in rat brain. *J Cereb Blood Flow Metab*, 13:125–134, 1993. doi:10.1038/jcbfm.1993.15.

[15] J. N. Rees et al. Protein reactivity of dopal depends on aldehyde catechol. *Chem Res Toxicol*, 22:1256–1263, 2009. doi:10.1021/tx9000557.

[16] J. A. Doorn et al. *ALDH inhibition generates a reactive aldehyde burden*. Free Radic Biol Med /, 2014. PMCID: PMC3932615.

[17] H. Cai et al. Aldh1 making molecular inroads into dopaminergic neurons. *Transl Neurodegener*, 3:2, 2014. PMCID: PMC4334846.

[18] A. Masato et al. Impaired dopamine metabolism dopal toxicity. *Mol Neurodegener*, 14:53, 2019. doi:10.1186/s13024-019-0332-6.

[19] H. Xu et al. Interplay of dopamine metabolism mitochondrial dysfunction. *Mol Psychiatry*, 27:4468–4483, 2022. doi:10.1038/s41398-022-02233-0.

[20] D. E. Edmondson. Hydrogen peroxide produced by mitochondrial mao catalysis: implications. *Curr Pharm Des*, 20:155–160, 2013. doi:10.2174/1381612811319099040 6.

[21] E. Lubos, J. Loscalzo, and D. E. Handy. Glutathione peroxidase-1 in health disease. *Antioxid Redox Signal*, 15:1957–1997, 2011. PMCID: PMC3159114.

[22] R. Dringen et al. Gpx is important for brain ho detoxification. *Brain Res.*, 759:67–75, 1997. doi:10.1016/S0006-8993(97)00233-3.

[23] A. K. Bouzier-Sore et al. Uncertainties in ppp flux in brain. *Front Neuroenergetics*, 7:10, 2015. PMCID: PMC4436897.

[24] B. Weber and L. F. Barros. The astrocyte: powerhouse recycling center. *Front Neuroenergetics*, 7:3, 2015. PMCID: PMC4665076.

[25] S. Takahashi and Y. Izawa. Neuroprotective function of high glycolytic activity in astrocytes (ppp $\rightarrow$ nadph $\rightarrow$ gsh). *Int J Mol Sci*, 22: 6568, 2021.

[26] K. Jomova et al. Antioxidant defense enzymes overview. *Arch Toxicol*, 98:1–39, 2024.

[27] P. Youssef et al. Ho consumption dominated by catalase/heme-peroxidases in brain homogenates. *Sci Rep*, 8:9481, 2018.

[28] M. F. Egan et al. Comt val158met effects on prefrontal function. *PNAS*, 98:6917–6922, 2001. doi:10.1073/pnas.111134598.

[29] D. Dickinson et al. Genes, cognition and brain through a comt lens. *Neurosci Biobehav Rev*, 33:1102–1113, 2009. PMCID: PMC2760675.

[30] R. M. Bilder et al. Relations to tonic-phasic da hypothesis comt val158met. *Neuropsychopharmacology*, 29:1943–1961, 2004.

[31] Y. N. Lamb et al. Comt val158met and cognition; met allele reduces activity 30–67.

[32] J. A. Best, H. F. Nijhout, and M. C. Reed. A mathematical model of da synthesis, release reuptake. *Theor Biol Med Model*, 6:21, 2009.

[33] S. Hoops et al. Copasi—a complex pathway simulator. *Bioinformatics*, 22:3067–3074, 2006.

[34] M. Hucka et al. Sbml level 3 version 2 core specification. *NPJ Syst Biol Appl*, 4:39, 2018. PMCID: PMC6167032.

[35] SciPy. documentation. solveivp for initial-value odes. (accessed 2025).

[36] I. M. Sobol. Global sensitivity indices for nonlinear models. *Math Comput Simul*, 55:271–280, 2001.